INTERNATIONAL JOURNAL FOR NUMERICAL METHODS IN FLUIDS
Int. J. Numer. Meth. Fluids 2006; **52**:987–1003
Published online 21 March 2006 in Wiley InterScience (www.interscience.wiley.com). DOI: 10.1002/fld.1218

Numerical analysis of mixed convection in three-dimensional rectangular channel with flush-mounted heat sources based on field synergy principle

Y. P. Cheng*,†, T. S. Lee‡ and H. T. Low§

Laboratory of Fluid Mechanics, Department of Mechanical Engineering, National University of Singapore, Singapore 119260, Singapore

SUMMARY

In this paper the fluid flow and heat transfer characteristics of mixed convection in three-dimensional rectangular channel with four heat sources are investigated numerically. The SIMPLEC algorithm is applied to deal with the coupling between pressure and velocity, and a new high-order stability-guaranteed second-order difference (SGSD) scheme is adopted to discretize the convection term. The influence of four parameters is studied: Richardson number, heat source distribution, channel height and inclination angle. The numerical results are analysed from the viewpoint of the field synergy principle, which says that the enhanced convective heat transfer is related not only to the velocity field and temperature field, but also to the synergy between them. It is found that the effects of the four parameters on the thermal performance can all be explained with the field synergy principle. To obtain better electronic cooling, the synergy between the velocity and temperature gradient should be increased when other conditions are unchanged. Copyright © 2006 John Wiley & Sons, Ltd.

KEY WORDS: mixed convection; numerical simulation; electronic cooling; field synergy principle

1. INTRODUCTION

With the rapid development of electronic technology, it is becoming a crucial problem to keep the electronic devices working reliably under the allowable temperature range. For every 2°C temperature rise, the reliability of a silicon chip will be decreased by about 10% [1]. Hence, thermal management issues have been widely investigated by many researchers. Due to its low cost and simplicity, air-cooling is preferred in the current cooling technology. Incropera [2] provided a comprehensive review on electronic equipment cooling and gave some suggestions

*Correspondence to: Y. P. Cheng, Laboratory of Fluid Mechanics, Department of Mechanical Engineering, National University of Singapore, Singapore 119260, Singapore.
†E-mail: g0402944@nus.edu.sg
‡E-mail: mpeleets@nus.edu.sg
§E-mail: mpelowht@nus.edu.sg

Received 17 October 2005
Revised 3 February 2006
Accepted 3 February 2006

for further research. Later Sathe and Sammakia [3] reviewed the recent developments in heat sink design and applications.

However, most research on electronic cooling is focused on forced convection. Because the cooling of electronic systems is mostly under the low-to-moderate Reynolds number regime, natural convection may also play an important role. Through the numerical simulation on mixed convection in multiple-layered boards, Kim *et al.* [4] found that due to the effect of buoyancy, the cooling efficiency in a vertically oriented channel is slightly higher than that in the horizontally oriented channel. Furthermore, through both experiments and numerical simulation, Mahaney *et al.* [5] pointed out that in horizontal rectangular channels with discrete heat sources, heat transfer due to mixed convection can be enhanced by a factor of three over that of forced convection, while the pumping power can be reduced. Therefore, mixed convection is gaining more and more attention.

Recently, Oztop and Dagtekin [6] and Guo and Sharif [7] numerically simulated mixed convection in a two-dimensional lid-driven square cavity. A comprehensive review on two-dimensional laminar mixed convection flow over backward-facing and forward-facing steps was conducted by Abu-Mulaweh [8], in which a detailed summary of the effect of several parameters on the flow and heat transfer was given. Iwai *et al.* [9] studied the effects of duct-inclination angle on the mixed convective flow over a backward-facing step with a three-dimensional model. Huang and Lin [10] applied the transient three-dimensional model to simulate the mixed convection flow in an inclined rectangular duct, and the flow transition and stability were also studied. Later Rahman and Raghavan [11] investigated the transient response of protruding electronic modules exposed to a horizontal cross flow, and found that Nusselt number is strongly dependent on the Fourier number and Richard number. Recently, Wang and Jaluria [12] studied the instability in mixed convection flow in a horizontal rectangular channel with multiple strip heat sources at low Reynolds numbers, and four different flow patterns were identified which can influence the fluid flow and heat transfer.

Besides the influence of some geometric parameters, the influence of heat source distribution was also addressed by several researchers. da Silva *et al.* [13, 14] studied the optimal distribution of discrete heat sources with the constructal theory for laminar forced convection and natural convection, respectively; their results show that the heat sources should be distributed non-uniformly with the smallest distance between the heat sources near the tip of the boundary condition. Chuang *et al.* [15] studied numerically the natural convection in a three-dimensional enclosure with three chips and five different position arrangements. Liu and Thien [16] found that to achieve the best thermal performance the conventional equi-spaced arrangement of chips is not preferred, while the centre-to-centre distances between chips should follow a geometric ratio, which is the golden mean (1.618). Chen *et al.* [17] proved this phenomenon by experiments and stated that when the geometric ratio is increased beyond 2.0, the thermal performance begins to decrease.

Both experiments and numerical simulation are the focus of this parametric study. The parameters studied involved the Reynolds number, Prandtl number, Richardson number, channel height, chip size, etc. By varying one of these parameters while keeping the others unchanged, the resultant friction and heat transfer performance are obtained. Also in this paper, these problems are revisited from a novel viewpoint—the field synergy principle, which can explain aspects of the above problems.

The field synergy principle was firstly proposed by Guo and co-workers [18, 19] in 1998 for the parabolic convective flow. This principle states that the heat transfer enhancement is

related not only to the velocity field and temperature field, but also to the synergy between them. The better the synergy, the higher the heat transfer rate. Later Tao *et al.* [20, 21] extended this idea to the elliptic flow when the fluid Peclet number is not too small. Guo *et al.* [22] applied this principle to the practical application.

This paper examines the effects of four typical parameters on fluid flow and heat transfer in a rectangular channel with four heating elements mounted on the bottom. The four parameters are Richardson number, heat source distribution, channel height and inclination angle. The synergy between the velocity and temperature field is indicated by the volume average intersection angle between velocity vector and temperature gradient. The numerical results show that the heat transfer variation, with the parameters studied, is consistent with the field synergy principle, i.e. the better the heat transfer, the smaller the average intersection angle, which means the better the synergy between velocity and temperature fields.

In the following, the physical model and mathematic formulation are proposed first, followed by the validation of the code and a mesh independence study. Then the influence of Richardson number, heat source, distribution, channel height and inclination angle on the heat transfer and friction are obtained numerically. The results are then explained from the viewpoint of the field synergy principle, and finally some conclusions are drawn which are helpful in the design of electronic cooling.

2. PHYSICAL MODEL AND MATHEMATICAL FORMULATION

The flow is assumed to be three-dimensional, steady, incompressible and laminar. Since the major task of the present study is to examine the feasibility of the field synergy principle in electronic cooling, some simplification is made in this study. The physical model is shown in Figure 1 and all the parameters are non-dimensional. Here x stands for the flow direction, with y and z being the width direction and height direction, respectively. The channel is rectangular with the length being 12 and width being 2, and the height may vary. The square heating sources are mounted at the bottom of the channel with the side length being 1. The cooling air flows into the channel from the left, and leaves from the right after being heated by the heat sources. Due to the temperature difference existing between the heating elements and flowing air, the air near the heating elements will be heated and rise due to buoyancy. Because of the interaction between the natural convection and forced convection, the flow in the channel becomes quite complex. In order to simulate the fluid flow and heat transfer accurately, a non-uniform grid is used in z direction, with a fine grid near the wall and coarse grid near the centre.

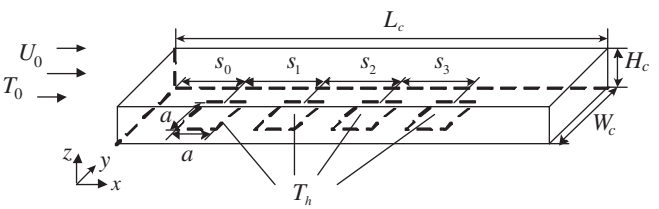

Figure 1. Schematic diagram of fluid flow in rectangular channel with four heat sources.

The non-dimensional equations for continuity, momentum and energy for the mixed convection in the channel are shown below:

Continuity equation

$$\frac{\partial U}{\partial X}+\frac{\partial V}{\partial Y}+\frac{\partial W}{\partial Z}=0 \tag{1}$$

Momentum equations

$$U\frac{\partial U}{\partial X}+V\frac{\partial U}{\partial Y}+W\frac{\partial U}{\partial Z}=-\frac{\partial P}{\partial X}+\frac{1}{Re}\left(\frac{\partial^2 U}{\partial X^2}+\frac{\partial^2 U}{\partial Y^2}+\frac{\partial^2 U}{\partial Z^2}\right)+RiT\sin\theta \tag{2a}$$

$$U\frac{\partial V}{\partial X}+V\frac{\partial V}{\partial Y}+W\frac{\partial V}{\partial Z}=-\frac{\partial P}{\partial Y}+\frac{1}{Re}\left(\frac{\partial^2 V}{\partial X^2}+\frac{\partial^2 V}{\partial Y^2}+\frac{\partial^2 V}{\partial Z^2}\right) \tag{2b}$$

$$U\frac{\partial W}{\partial X}+V\frac{\partial W}{\partial Y}+W\frac{\partial W}{\partial Z}=-\frac{\partial P}{\partial Z}+\frac{1}{Re}\left(\frac{\partial^2 W}{\partial X^2}+\frac{\partial^2 W}{\partial Y^2}+\frac{\partial^2 W}{\partial Z^2}\right)+RiT\cos\theta \tag{2c}$$

Energy equation

$$U\frac{\partial T}{\partial X}+V\frac{\partial T}{\partial Y}+W\frac{\partial T}{\partial Z}=\frac{1}{RePr}\left(\frac{\partial^2 T}{\partial X^2}+\frac{\partial^2 T}{\partial Y^2}+\frac{\partial^2 T}{\partial Z^2}\right) \tag{3}$$

where Re is defined with the side length a of the heating elements; $Ri=Gr/Re^2$, is a non-dimensional number which indicates the relative strength of natural convection and forced convection; θ is the angle between the streamwise direction and horizontal direction, which ranges from -90° to 90° in this study.

Because the governing equations are elliptic, all the boundary conditions are required for the computational domain, which are as follows:

$$\text{At the inlet:}\quad U=U_{\text{Dev}},\quad V=0\quad W=0\quad T=0 \tag{4a}$$

$$\text{At the outlet:}\quad \frac{\partial U}{\partial X}=\frac{\partial V}{\partial X}=\frac{\partial W}{\partial X}=\frac{\partial T}{\partial X}=0 \tag{4b}$$

$$\text{At the wall:}\quad U=V=W=0 \tag{4c}$$

$$\begin{aligned}&\text{(a) At the heat sources: } T=1\\&\text{(b) At other region: adiabatic condition}\end{aligned} \tag{4d}$$

U_{Dev} is the developed velocity, which can be obtained through the preliminary computation by setting the periodic boundary conditions in x direction for forced convection.

The governing equations are discretized with a finite volume method [23]. According to Zeng and Tao [24], considering the computational time needed and robustness, the SIMPLEC algorithm owns the best comprehensive performance for fine grids among the SIMPLE-family of algorithms; hence, it is adopted here to deal with the coupling between the pressure and velocity terms. The convergence criterion is that the maximum mass residual of the cells divided by the inlet mass flow is less than 1.0×10^{-8}. In order to obtain an accurate solution,

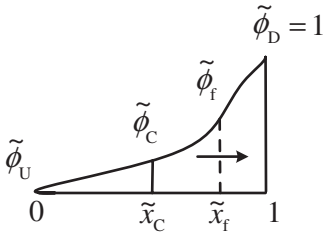

Figure 2. Normalized variable and profile.

the high-order stability-guaranteed second-order difference (SGSD) scheme [25] is adopted which is formulated based on the central difference (CD) and second-order upwind difference (SUD). With the normalized variable and space formulation methodology shown in Figure 2, the scheme can be expressed as

$$\tilde{\phi}_f = \beta\tilde{\phi}_f^{\mathrm{CD}} + (1-\beta)\tilde{\phi}_f^{\mathrm{SUD}} = \beta\left(\frac{\tilde{x}_f - \tilde{x}_C}{1-\tilde{x}_C} + \frac{\tilde{x}_f - 1}{\tilde{x}_C - 1}\,\tilde{\phi}_C\right) + (1-\beta)\frac{\tilde{x}_f}{\tilde{x}_C}\,\tilde{\phi}_C \tag{5}$$

β is a variable which is determined according to relative strength of convection and diffusion and is defined as

$$\beta = \frac{2}{2 + |P_\Delta|} \tag{6}$$

where P_Δ is the local grid Peclet number.

3. RESULTS AND DISCUSSION

In this paper, the following parameters are defined as

$$\text{The local Nusselt number:} \quad Nu(x,y) = -\left.\frac{\mathrm{d}T}{\mathrm{dZ}}\right|_{\text{heat source}} \tag{7}$$

$$\text{The average Nusselt number:} \quad Nu = \iint_A Nu(x,y)\,\mathrm{d}x\,\mathrm{d}y/A \tag{8}$$

$$\text{Fraction factor:} \quad f = \frac{2\Delta P\, a}{L_c} \tag{9}$$

$$\text{Local intersection angle:} \quad \alpha = \cos^{-1}\left(\frac{\mathbf{U}\nabla T}{|\mathbf{U}\nabla T|}\right) \tag{10}$$

$$\text{Average intersection angle:} \quad \alpha_m = \frac{\sum \alpha_{i,j,k}\Delta V_{i,j,k}}{\sum \Delta V_{i,j,k}} \tag{11}$$

It is notable that when the local intersection angle α is greater than 90°, it is replaced by $180° - \alpha$ in the calculation of average intersection angle. Here for convenience of discussion, the intersection angle is called the synergy angle hereafter.

Table I. Comparison with benchmark solutions.

	$Ra = 10^4$			$Ra = 10^5$			$Ra = 10^6$		
	U_{max}	V_{max}	Nu	U_{max}	V_{max}	Nu	U_{max}	V_{max}	Nu
Wakashima	0.198	0.222	2.062	0.142	0.246	4.367	0.081	0.258	8.697
Present results	0.198	0.224	2.051	0.143	0.245	4.342	0.080	0.263	8.686
Relative deviation	−0.01%	1.13%	−0.52%	1.13%	−0.61%	−0.56%	−0.84%	1.94%	−0.13%

3.1. Validation of the code and mesh independence of solution

To validate the code developed with the high scheme SGSD and SIMPLEC algorithm, preliminary computations were first conducted for the three-dimensional natural convection in a cube with two opposite walls differentially heated with the others being adiabatic. The benchmark solutions were offered by Wakashima and Saitoh [26] with the high-order time-space method. In their numerical simulation the uniform grid number $120 \times 120 \times 120$ in space was used while in this paper the non-uniform grid $62 \times 62 \times 62$ is used. Here two maximum velocities and average Nusselt number are compared under different Ra numbers, as shown in Table I. From this table, we can see that the maximum deviation between the predicted results and the benchmark solutions is within 2%. The good agreement shows the reliability of code.

In order to adopt an appropriate grid system, a grid-independence study is conducted to investigate the influence of the grid density on the computational results. The pure forced convection in the rectangular channel at $Re = 500$ is modelled with the developed velocity and developing temperature. Five different grid systems $62 \times 18 \times 16$, $62 \times 22 \times 22$, $92 \times 32 \times 22$, $122 \times 42 \times 22$ and $152 \times 52 \times 22$ are used. The numerical results for friction factor and Nusselt number are shown in Figures 3 and 4. Compared to the finest grid $152 \times 52 \times 22$, the grid $62 \times 22 \times 22$ yields about 0.5% lower friction factor and Nusselt number. Hence, in order to save computer resources the grid system $62 \times 22 \times 22$ is adopted for the following numerical simulations.

With the increase in Reynolds number, the flow may become unsteady. Therefore, the steady and unsteady models are compared here for the forced convection in the rectangular channel with the highest Reynolds number of 1000. A fully implicit scheme was used for the unsteady computation; the time step was taken as 0.1, which is small enough to catch any oscillation during the time marching procedure. From Figure 5 we can see that the non-dimensional pressure drop approaches a constant 0.669, only 0.45% higher than the value with the steady model. Meanwhile, the Nusselt number 13.53 from the unsteady model is only 0.37% lower than 13.58 obtained with the steady model. Because the unsteady computation is very time-consuming, the comparison above shows that the steady model is acceptable and reliable, hence it is adopted in the following computations.

In the following calculation, the effects of Richardson number, channel height, heat source distribution and inclination angle are investigated. For each examination, only one parameter varies while all the other conditions remain the same. The base case is that the channel height is one fourth of the spanwise width, heat sources are distributed uniformly at the bottom of the channel and inclination angle is zero.

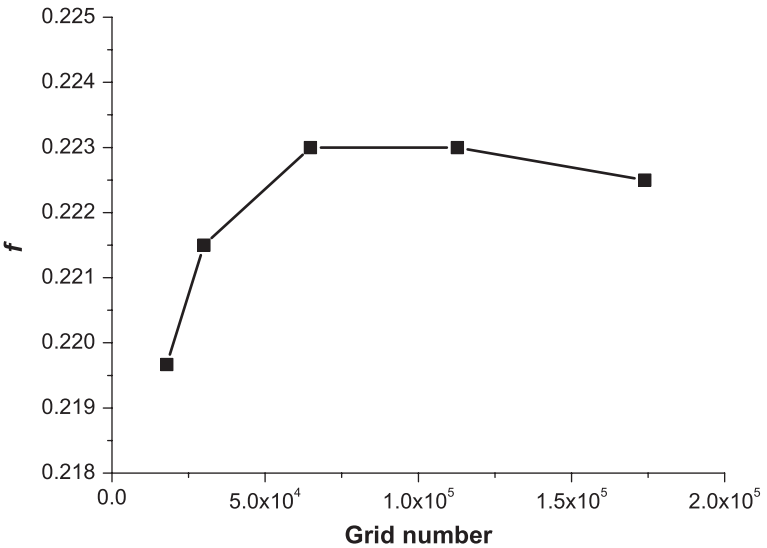

Figure 3. Friction factor variation with grid number.

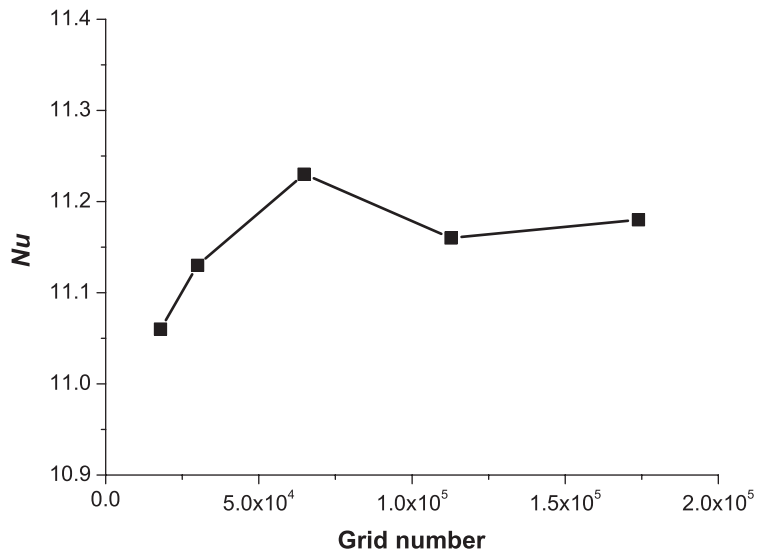

Figure 4. Nusselt number variation with grid number.

3.2. Influence of Richardson number

In the mixed convection flow, due to the existence of natural convection, the flow and heat transfer performance are greatly influenced. In Figures 6 and 7, the friction factor and Nusselt

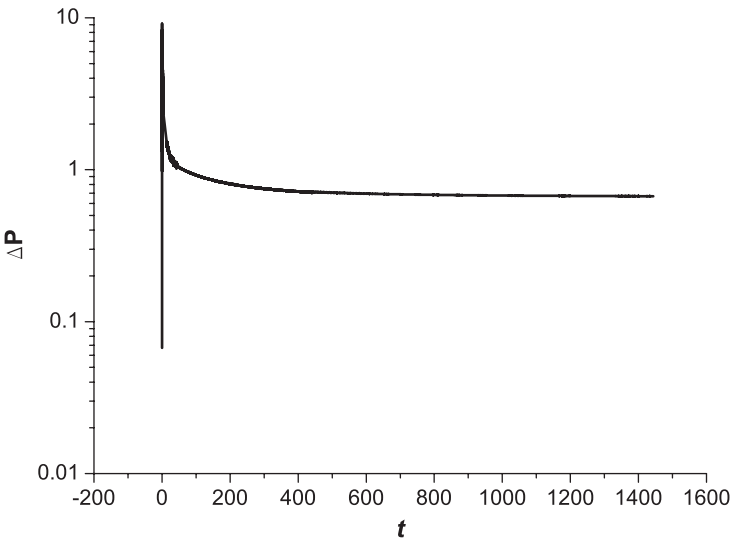

Figure 5. Time course of non-dimensional pressure drop.

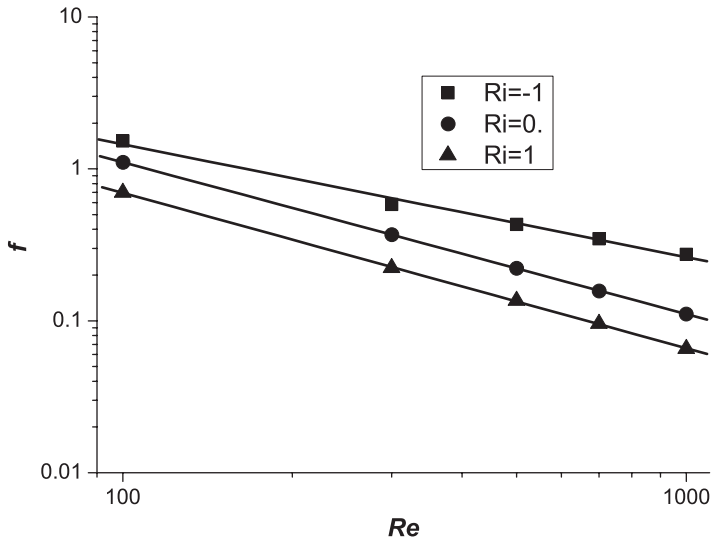

Figure 6. Friction factor variation with *Re* under difference *Ri*.

number are shown under different *Ri* numbers. It is noted that the negative value of *Ri* means that buoyant force is opposite that of the forced convection direction; while the positive value of *Ri* stands for the buoyancy assisted flow. As we expect, the friction factor decreases while the Nusselt number increases with the increasing Reynolds number. When $Ri = -1$, due to the opposing effect, the buoyant forces retard the air in the channel and the friction factor is much

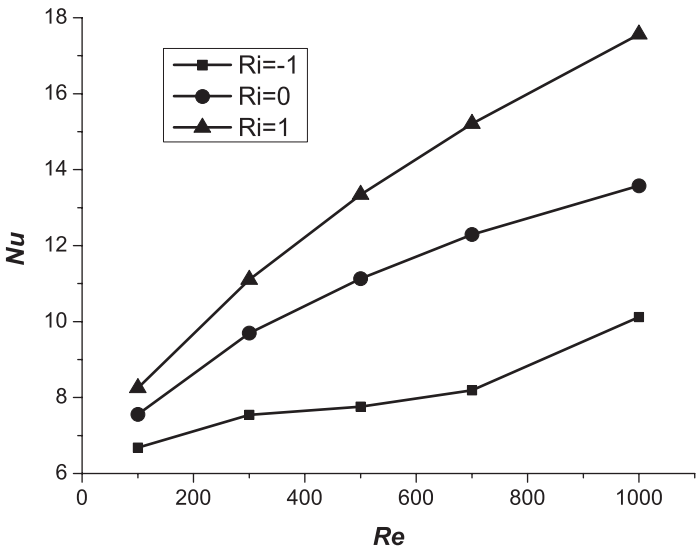

Figure 7. *Nu* variation with *Re* under different *Ri*.

larger than that of the pure forced convection when $Ri = 0$. Furthermore, the buoyant forces also weaken the heat transfer between the heating elements and air. However, when $Ri = 1$, the case is opposite. Hence, in electronic cooling, the coolant flow should be buoyant-aiding in order to attain the better performance, which cannot only enhance the heat transfer, but also can reduce the needed power of cooling fans.

Because $Ri = Gr/Re^2$, when the Reynolds number is quite low, the natural convection is also very weak, and the influence of buoyant forces on the forced convection is also weak. For example, when $Re = 100$, the Nusselt number of the buoyant-opposing flow is 11.6% lower than that of forced convection, and the buoyant-aiding flow is 9.2% higher than that of the forced convection. While with the increase in *Re* number, the *Gr* number increases more rapidly, the influence of the buoyant forces on the forced convection become larger. At $Re = 1000$, the buoyant-opposing flow has a 25.5% lower Nusselt number while the buoyant-aiding flow has a 29.3% higher Nusselt number than that of forced convection. Meanwhile, the friction factor of the buoyant-opposing flow is nearly 1.5 times higher than that of forced convection, while at $Re = 100$, it is only 38% higher.

It is notable that when $Ri = 0$, the flow is a developed forced convection in the rectangular channel, hence the value of fRe should be a constant. If the hydraulic diameter of the channel is taken as the characteristic length, the calculated fRe is 70.5, much close to the theoretical value 73 [27]. Figure 8 shows the velocity distribution in the mid-plane in *y* direction when $Ri = -1$, from which we can see why the thermal performance is reduced in the buoyant-opposing flow. At the inlet, due to the fully developed flow, the distribution of velocity is parabolic, while near the heating sources at the bottom, some vortices appear which weaken the heat transfer between the heating sources and the incoming flow. However, for the buoyant-aiding flow, the boundary layer near the heating sources will be greatly reduced which leads to the better thermal performance.

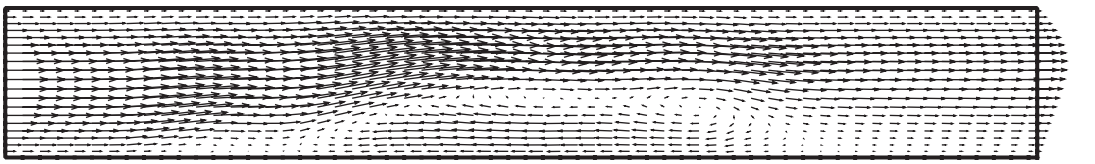

Figure 8. Velocity distribution at the mid-plane in y direction at $Re = 500$, $Ri = -1$.

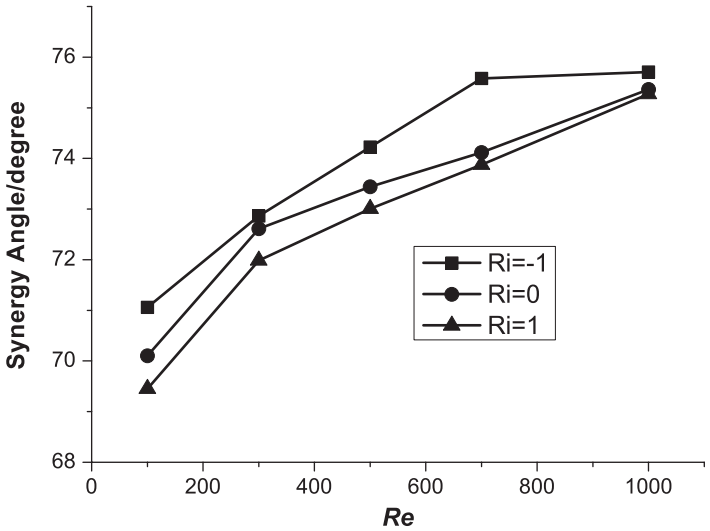

Figure 9. Synergy angle variation with Re under different Ri.

The above explanation is based on the traditional viewpoints, which cannot reveal the essence of enhanced heat transfer. Here we can apply the field synergy principle to explain this result. For three cases the Nusselt number increases with the increasing Reynolds number, as seen from Figure 7. However, from Figure 9 we can see that with the increase in Re number, the synergy angles for three cases also increase, which means the synergy between the velocity and temperature field becomes worse; hence, the increase rate of Nusselt numbers becomes mild as we expect. It can also be seen that the synergy angle of buoyant-opposing flow is always larger while the buoyant-aiding flow is less than that of forced convection flow when $Ri = 0$, which indicates that the synergy between velocity and temperature field in buoyant-opposing flow is the worst situation, and thus results in the lowest Nusselt number among three cases. For the buoyant-aiding flow the case is opposite. From this analysis we know that the field synergy principle can be used to explain the difference in thermal performance among three cases with different Richardson numbers.

3.3. Influence of heating source distribution

The distribution of heating sources also has a great influence on the heat transfer with the other conditions unchanged. In this study the centre-to-centre distance between the adjacent heating

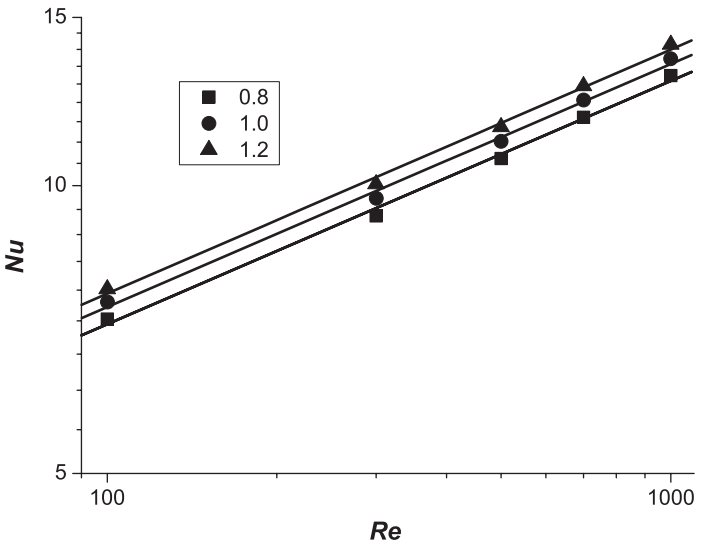

Figure 10. *Nu* variation with *Re* under different geometric ratio.

sources follows a certain geometric ratio along the x direction, i.e. $s_2/s_1 = s_3/s_2 =$ constant, and the forced convection with three different geometric ratios 0.8, 1.0 and 1.2 was investigated. The Nusselt number variation with Reynolds number for these three cases is shown in Figure 10. Within the range of the considered Reynolds number, the heat source distribution with geometric ratio 0.8 shows about 4% lower *Nu* than that with equi-spaced arrangement, while when the geometric ratio is 1.2, it is nearly 3.5% higher than that with equi-spaced arrangement. From the traditional viewpoint it is difficult to explain this phenomenon. However, the field synergy principle can explain this. From Figure 11 we can see that the synergy angle of the heat source distribution for the geometric ratio 0.8 is the greatest among the three cases, while that of the heat source distribution for the geometric ratio 1.2 is the least. The smaller the average synergy angle, the better the thermal performance, hence when the geometric ratio is 1.2, the Nusselt number is the highest. Although the difference of synergy angle among three cases is quite small, even less than 1 degree, its cosine value difference can be quite large. For example, at $Re = 100$, the cosine value of synergy angle when the geometric ratio equals to 0.8 is nearly 3% higher than that when geometric ratio is 1.2.

It is noted that the Nusselt number is proportional to $Re^{1/4}$ when the heating sources are at a uniform temperature, while when the heating sources have a uniform heat flux, the Nusselt number can be higher, which is proven by Tso *et al.* [28]. In their experimental study, the Nusselt number is proportional to $Re^{1/3}$ for the laminar forced convection.

3.4. Influence of channel height

When the heating sources have a uniform heat flux, the channel height has little effect on the overall thermal performance, and the flow can be considered as an external flow [28]. However, the channel height has a significant influence on the thermal performance when the heat sources are at a constant temperature. In this study the channel height H varies from

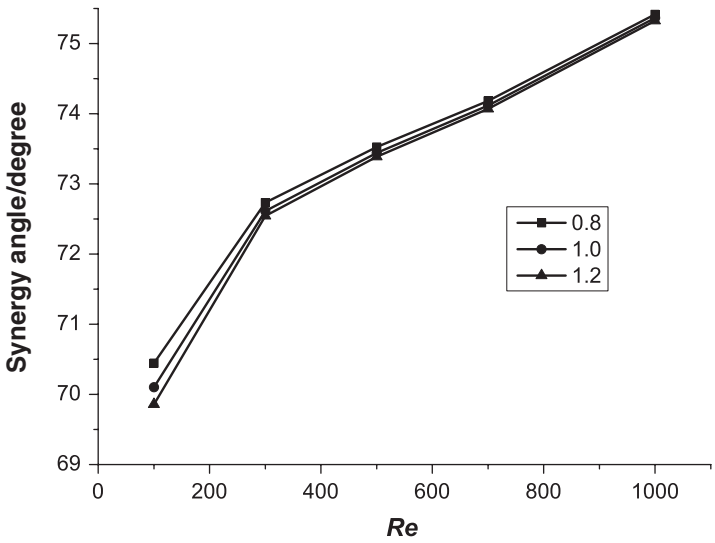

Figure 11. Synergy angle variation with *Re* under different geometric ratio.

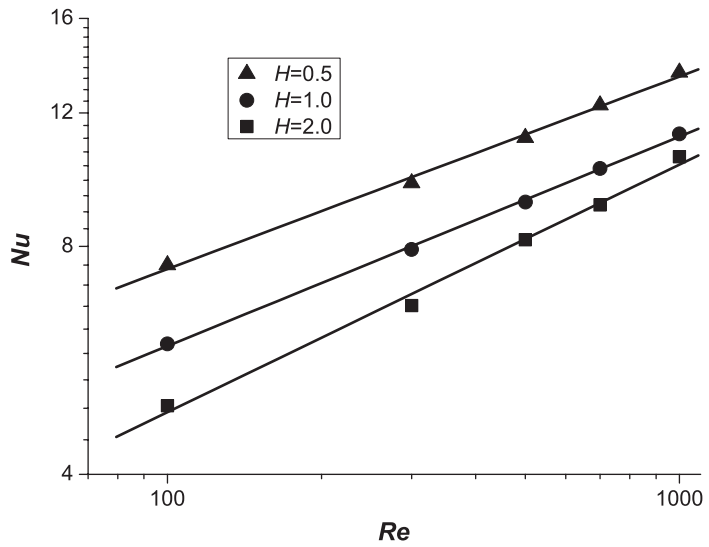

Figure 12. *Nu* variation with *Re* under different channel height.

0.5 to 2.0. From Figure 12 we can see that the smaller the channel height, the higher the overall Nusselt number. When the channel height is 0.5 the Nusselt number is 53% higher at $Re = 100$ and 29% higher at $Re = 1000$, respectively, than that when the channel height is 2.0. The influence of the channel height on the friction factor is more pronounced than that on

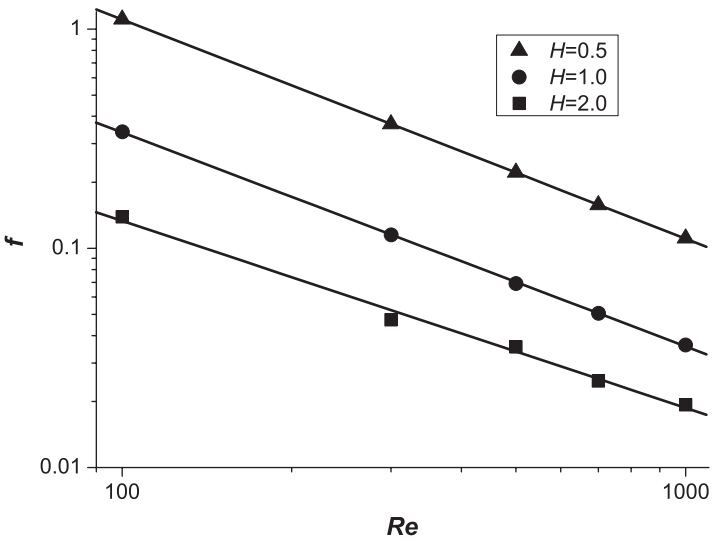

Figure 13. Friction factor f variation with Re under different channel height.

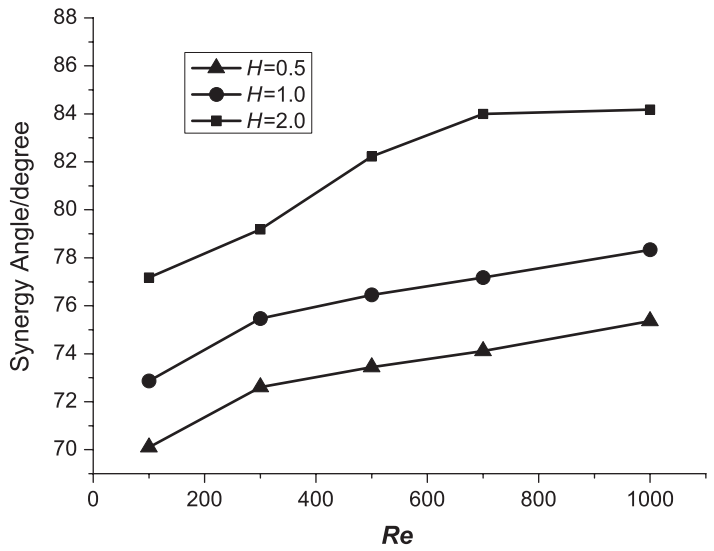

Figure 14. Synergy angle variation with Re under different channel height.

the Nusselt number. With the length of heating sources as the characteristic length, as seen from Figure 13, the friction factor is nearly 6 times higher at $Re = 100$ when channel height is 0.5 than that when the channel height is 2.0. With the increase in Reynolds number, it is about 3.7 times higher.

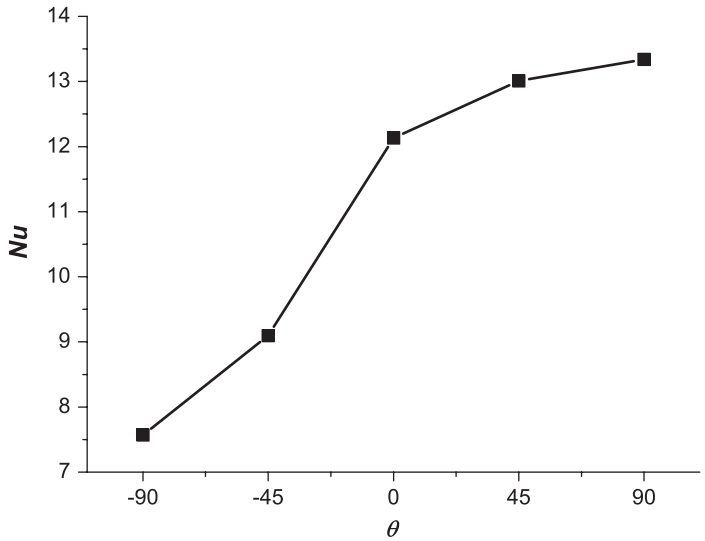

Figure 15. *Nu* variation with inclination angle.

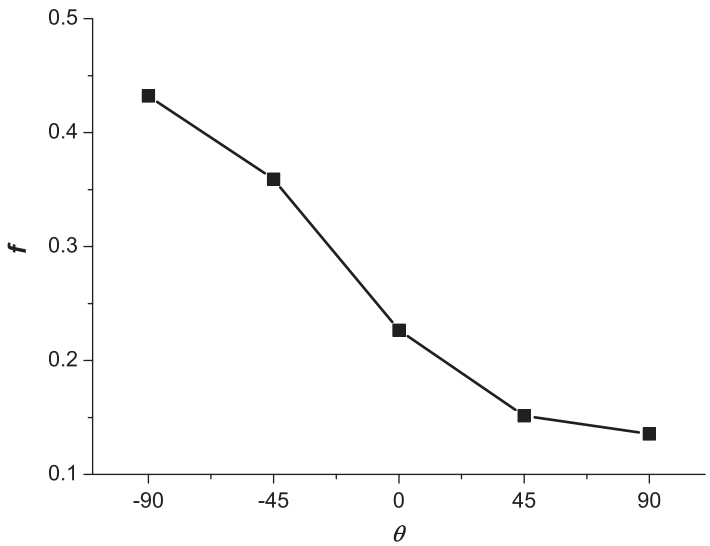

Figure 16. Friction factor variation with inclination angle.

The large differences in Nusselt numbers with different channel height can be attributed to the different synergy angles. From Figure 14 we see that with the increase in channel height, the synergy angle increases too, which indicates that the synergy between velocity and temperature field is reduced, and thus the Nusselt number is decreased correspondingly.

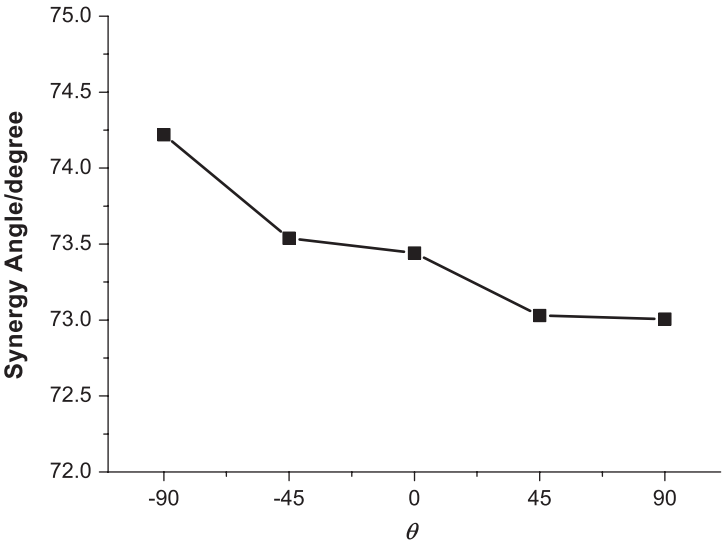

Figure 17. Synergy angle variation with inclination angle.

3.5. *Influence of inclination angle*

Figures 15 and 16 show the influence of inclination angle on the Nusselt number and friction factor, respectively, at $Ri = 1$. The inclination angle θ is defined as the angle between the inlet flow direction and horizontal line, which ranges from $-90°$ to $90°$. At $\theta = -90°$, the air flows downward along the channel, hence it is a buoyant-opposing flow; at $\theta = 90°$, it becomes a buoyant-aiding flow. Therefore, with the increase in inclination angle, the Nusselt number increases, but the friction factor decreases. When $\theta < 0$, the influence of the inclination angle on Nusselt number is quite great. For example, when the inclination angle θ increases from $-90°$ to 0, the Nusselt number is increased by 60% from 7.6 to 12.1, while when θ increases from 0 to $90°$, the Nusselt number is increased only by 10% from 12.1 to 13.3. The friction factor is also reduced greatly with the increase in inclination angle, but when $\theta \geqslant 45°$ the friction factor begins to vary little. Therefore, in order to attain the better thermal and friction performance, the inclination angle is recommended to be greater than $45°$.

From Figure 17 we can also see that the synergy angle decreases with the increase in inclination angle, which again shows that when the synergy between velocity and temperature field improves, the heat transfer is enhanced.

4. CONCLUSION

In this article the three-dimensional laminar mixed convection flow in a rectangular channel is simulated numerically. The influence of Richardson number, heating source distribution, channel height and inclination angle on the overall thermal and friction performance is obtained, and also is analysed with the aid of the field synergy principle. The major findings

are summarized as follows:

1. With the increase in Richardson number, the friction factor will decrease while the Nusselt number increases. The Richardson number has more influence on the friction factor and Nusselt number at high Reynolds number.
2. When the geometric ratio for heating source distribution is greater than 1, better thermal performance can be obtained.
3. Channel height has great influence on the overall Nusselt number and friction factor when the heating sources are at constant temperature. With the increase in channel height, the Nusselt number and friction factor will decrease greatly.
4. In order to obtain a better thermal and friction factor, the inclination angle of the channel had better be greater than 45°.
5. The influence of the four parameters above on the thermal performance can all be analysed with the field synergy principle, which proves the reliability of this principle in enhancing heat transfer.

REFERENCES

1. Bar-Cohen A, Kraus AD, Davidson SF. Thermal frontiers in the design and packaging of microelectronic equipment. *Mechanical Engineering*. 1983; **105**(6):53–59.
2. Incropera FP. Convection heat transfer in electronic equipment cooling. *Journal of Heat Transfer* (ASME) 1988; **110**:1097–1111.
3. Sathe S, Sammakia B. A review of recent developments in some practical aspects of air-cooled electronic packages. *Journal of Heat Transfer* (ASME) 1998; **120**:830–839.
4. Kim SY, Sung HJ, Hyun JM. Mixed convection from multiple-layered boards with cross-streamwise periodic boundary conditions. *International Journal of Heat and Mass Transfer* 1992; **35**(11):2941–2952.
5. Mahaney HV, Incropera FP, Ramadhyani S. Comparison of predicted and measured mixed convection heat transfer from an array of discrete sources in a horizontal rectangular channel. *International Journal of Heat and Mass Transfer* 1990; **33**(6):1233–1245.
6. Oztop HF, Dagtekin I. Mixed convection in two-sided lid-driven differentially heated square cavity. *International Journal of Heat and Mass Transfer* 2004; **47**:1761–1769.
7. Guo GH, Sharif MAR. Mixed convection in rectangular cavities at various aspect ratios with moving isothermal sidewalls and constant flux heat source on the bottom wall. *International Journal of Thermal Sciences* 2004; **43**:465–475.
8. Abu-Mulaweh HI. A review of research on laminar mixed convection flow over backward- and forward-facing steps. *International Journal of Thermal Sciences* 2003; **42**:897–909.
9. Iwai H, Nakabe K, Suzuki K, Matsubara K. The effects of duct inclination angle on laminar mixed convective flows over a backward-facing step. *International Journal of Heat and Mass Transfer* 2000; **43**:473–485.
10. Huang CC, Lin TF. Numerical simulation of transient aiding mixed convective air flow in a bottom heated inclined rectangular duct. *International Journal of Heat and Mass Transfer* 1996; **39**(8):1697–1710.
11. Rahman MM, Raghavan J. Transient response of protruding electronic modules exposed to horizontal cross flow. *International Journal of Heat and Fluid Flow* 1999; **20**:48–59.
12. Wang QH, Jaluria Y. Instability and heat transfer in mixed convection flow in a horizontal duct with discrete heat sources. *Numerical Heat Transfer*, *Part A* 2002; **42**:445–463.
13. da Silva AK, Lorente S, Bejan A. Optimal distribution of discrete heat sources on a plate with laminar forced convection. *International Journal of Heat and Mass Transfer* 2004; **47**:2139–2148.
14. da Silva AK, Lorenzini G, Bejan A. Distribution of heat sources in vertical open channels with natural convection. *International Journal of Heat and Mass Transfer* 2005; **48**:1462–1469.
15. Chuang SH, Chiang JS, Kuo YM. Numerical simulation of heat transfer in a three-dimensional enclosure with three chips in various position arrangements. *Heat Transfer Engineering* 2003; **24**(2):42–59.
16. Liu Y, Thien NP. An optimum spacing problem for three chips mounted on a vertical substrate in an enclosure. *Numerical Heat Transfer*, *Part A* 2000; **37**:613–630.
17. Chen S, Liu Y, Chan SF, Leung CW, Chan TL. Experimental study of optimum spacing problem in the cooling of simulated electronic package. *Heat and Mass Transfer* 2001; **37**:251–257.
18. Guo ZY, Li DY, Wang BX. A novel concept for convective heat transfer enhancement. *International Journal of Heat and Mass Transfer* 1998; **41**:2221–2225.

19. Wang S, Li ZX, Guo ZY. Novel concept and device of heat transfer augmentation. *Proceedings of the 11th International Conference of Heat Transfer*, Philadelphia, U.S.A. Taylor & Francis: Bristol, PA, 1998; 405–408.
20. Tao WQ, Guo ZY, Wang BX. Field synergy principle for enhancing convective heat transfer—its extension and numerical verifications. *International Journal of Heat and Mass Transfer* 2002; **45**:3849–3856.
21. Tao WQ, He YL, Wang QW, Qu ZG, Song FQ. A unified analysis on enhancing single phase convective heat transfer with field synergy principle. *International Journal of Heat and Mass Transfer* 2002; **45**(24): 4871–4879.
22. Guo ZY, Tao WQ, Shah RK. The field synergy (coordination) principle and its applications in enhancing single phase convective heat transfer. *International Journal of Heat and Mass Transfer* 2005; **48**:1797–1807.
23. Patankar SV. *Numerical Heat Transfer and Fluid Flow*. McGraw-Hill: New York, 1980.
24. Zeng M, Tao WQ. A comparison study of the convergence characteristics and robustness for four variants of SIMPLE-family at fine grids. *Engineering Computations* 2003; **20**:320–340.
25. Li ZY, Tao WQ. A new stability-guaranteed second-order difference scheme. *Numerical Heat Transer*, *Part B*, 2002; **42**:349–365.
26. Wakashima S, Saitoh TS. Benchmark solutions for natural convection in a cubic cavity using the high-order time-space method. *International Journal of Heat and Mass Transfer* 2004; **47**:853–864.
27. Shah RK, London AL. Laminar flow forced convection in ducts. *Advances in Heat Transfer*, Supplement No. 1. Academic Press: New York, 1978.
28. Tso CP, Xu GP, Tou KW. An experimental study on forced convection heat transfer from flush-mounted discrete heat sources. *Journal of Heat Transfer* (ASME) 1999; **121**:326–332.

